TRR
JOURNAL OF THE TRANSPORTATION RESEARCH BOARD

Research Article

Transportation Research Record
1–16

DOI: 10.1177/03611981221094822
journals.sagepub.com/home/trr
SAGE

Impact of Cooperative Adaptive Cruise Control on Traffic Stability

Yun-Chu Hung[1] and Kuilin Zhang[1]

Abstract

Cooperative adaptive cruise control (CACC) is one of the popular connected and automated vehicle (CAV) applications for cooperative driving automation with combined connectivity and automation technologies to improve string stability. This study aimed to derive the string stability conditions of a CACC controller and analyze the impacts of CACC on string stability for both a fleet of homogeneous CAVs and for heterogeneous traffic with human-driven vehicles (HDVs), connected vehicles (CVs) with connectivity technologies only, and autonomous vehicles (AVs) with automation technologies only. We mathematically analyzed the impact of CACC on string stability for both homogeneous and heterogeneous traffic flow. We adopted parameters from literature for HDVs, CVs, and AVs for the heterogeneous traffic case. We found there was a minimum constant time headway required for each parameter design to ensure stability in homogeneous CACC traffic. In addition, the constant time headway and the length of control time interval had positive correlation with stability, but the control parameter had a negative correlation with stability. The numerical analysis also showed that CACC vehicles could maintain string stability better than CVs and AVs under low HDV market penetration rates for the mixed traffic case.

Keywords

Cooperative adaptive cruise control (CACC), Connected and automated vehicles (CAV), Cooperative driving automation, string stability, mixed traffic

Connectivity and automation technologies in connected and automated vehicles (CAVs) have the potential to improve safety, mobility, and the environment in transportation systems. Cooperative adaptive cruise control (CACC) is one of the popular CAV applications for cooperative driving automation with combined connectivity and automation technologies that can improve string stability (*1*, *2*). String stability is concerned with how a fluctuation in motion is propagated through a platoon of vehicles (*3*, *4*). Based on the stability function by Ward (*5*), Talebpour and Mahmassani studied the impact of connected vehicles (CVs, i.e., with connectivity technology only) and autonomous vehicles (AVs, i.e., with automation technology only) in mixed traffic with human-driven vehicles (HDVs) on string stability (*6*). However, quantifying the impact of cooperative driving automation in CAVs (i.e., with combined connectivity and automation technologies such as CACC) on string stability has yet to be explored. Therefore, the objective of this study was to derive the string stability conditions of a CACC controller and analyze the impacts of CAVs on string stability for both a fleet of homogeneous CAVs and on heterogeneous traffic with HDVs, CVs, AVs, and CAVs.

String stability has been analyzed to evaluate CAV controllers' performance (*7*–*13*). Sun et al. comprehensively reviewed four methods for string stability in car-following models (*14*). Feng et al. reviewed and presented the relationships of the original and several modified string stability definitions (*15*). For homogeneous traffic flow, several CACC controller designs have been proposed with string stability to ensure oscillations are not amplified to upstream traffic flows (*16*–*23*). However, in the heterogeneous driving environment, although the stability of mixed CACC traffic flow has been investigated by Li and Wang (*24*) and Qin and Li (*25*), neither studies simultaneously compared the stability improvements of CACC vehicles in relation to different market penetration rates (MPRs) and more vehicle types. In this paper,

[1]Department of Civil, Environmental, and Geospatial Engineering, Michigan Technological University, Houghton, MI

Corresponding Author:
Kuilin Zhang, klzhang@mtu.edu

HDVs, CVs, AVs, and CAVs are discussed and compared under different MPRs.

This study focused on the impact of CAVs (with CACC controllers) on string stability for both homogeneous and heterogeneous traffic flow. We first derived the stability condition for a CACC controller from research by Milanés and Shladover (*26*) based on the transfer function method in a homogeneous CAV traffic environment. We also conducted a stability analysis of control parameters based on the stability conditions. To investigate the impact of CACC on string stability under heterogeneous traffic, we explicitly defined string stable and partially stable conditions by applying the stability function (*5*) and the critical speed concept developed in research by Talebpour and Mahmassani (*6*). The speed threshold (i.e., critical speed) in which traffic becomes unstable was used as a stability indicator to define three stability regions in control parameter analysis: absolutely stable-, conditionally stable-, and absolutely unstable regions. The numerical analysis showed that CAVs could maintain string stability better than CVs and AVs under low HDV MPRs.

This study makes two significant contributions. First, we derived the stability condition for the CACC model proposed by Milanés and Shladover (*26*) in a homogeneous CAV driving environment. The stability conditions provided a mathematically theoretical foundation for controller parameter design and stability analysis. We found a minimum constant time headway was required for each parameter design to ensure stability. In addition, the constant time headway and the length of the control time interval had a positive correlations with stability, but the control parameter had a negative correlation with stability. Second, using the stability function proposed by Ward (*5*) and the stability analysis presented in research by Talebpour and Mahmassani for heterogeneous traffic (*6*), we explicitly quantified the impact of CACC on string stability in heterogeneous traffic with HDVs, CVs, and AVs. The numerical analysis showed that CACC vehicles could maintain string stability better than CVs and AVs under low HDV MPRs.

The remainder of this paper is organized as follows: the next section introduces the acceleration models we adopted to model HDVs, CVs, AVs, and CAVs. The stability condition for a fleet of homogeneous CACC vehicles is then derived, and a stability analysis is conducted. This is followed by a stability analysis of heterogeneous traffic flow with HDVs, CVs, AVs, and CAVs. Finally, we present our conclusions.

Model Formulations

In this section, we introduce four acceleration model formulations for HDVs, CVs, AVs, and CAVs, respectively. We adopted the same HDV, CV, and AV models as Talebpour and Mahmassani (*6*). We choose a CACC model by Milanés and Shladover (*26*) for CAVs.

Human-Driven Vehicles

Considering that decision making is a cognitive behavior based on selecting an action from several alternatives, Hamdar et al. presented an acceleration framework that adapted prospect theory (PT) to model car-following behavior (*27*). PT postulates editing and evaluating in two phases (*28*). In the first phase, the model assigns the utility values to the effective alternatives and then evaluates the alternatives in the second phase. The following PT value function, $U_{PT}(a_n)$, is used to transform the "objective" utility into a perceived "subjective" value:

$$U_{PT}(a_n) = \frac{\left[w_m + (1 - w_m)\left(\tanh\left(\frac{a_n}{a_0}\right) + 1\right)\right]}{2} \Bigg/ \left[\frac{a_n}{(1 + a_n)^{\left(\frac{\gamma-1}{2}\right)}}\right] \tag{1}$$

where
a_n is the acceleration decision for driver n;
exponent of the PT utility, $\gamma>0$, and weighting factor, w_m, are parameters; and
a_0 normalizes the acceleration.
At each evaluation stage, a driver determines the behavior based on evaluating candidate acceleration alternatives. It assumes that drivers optimally choose the acceleration
function with the higher value. The total utility function of acceleration then has the following form:

$$U(a_n) = (1 - p_{n,i})U_{PT}(a_n) - p_{n,i}w_c k(v, \Delta v) \tag{2}$$

where
$p_{n,i}$ = crash probability of acceleration instance, i, for driver n;
w_c = crash weighting parameters; and
$k(v, \Delta v)$ = crash seriousness term, respectively.
To reflect the stochastic response adopted by the drivers, Hamdar calculated the probability density function (*29*),

$$f(a_n) = \begin{cases} \dfrac{e^{\beta_{PT}U(a_n)}}{\int_{a_{min}}^{a_{max}} e^{\beta_{PT}U(a')}da'}, & a_{min} < a_n < a_{max} \\ 0, & \text{otherwise} \end{cases} \tag{3}$$

where β_{PT} reflects the sensitivity of choice to the utility $U(a_n)$, and a_{min} and a_{max} are the minimum and maximum accelerations, respectively. We used this model for HDVs with the same parameter values as employed by Talebpour and Mahmassani (*6*).

Connected Vehicles

Assuming that CVs can share information with other vehicles and infrastructure, drivers can determine their driving behavior from receiving information in this connected environment. Based on capturing more realistic congestion dynamics than other acceleration modeling frameworks, the intelligent driver model (IDM) (*30*, *31*) was used to model the CVs with the same vehicle-to-vehicle and vehicle-to-infrastructure communication assumptions as in Talebpour and Mahmassani (*6*),

$$a^n_{IDM}(s_n,\ v_n,\ \Delta v_n) = \bar{a}_n\left[1 - \left(\frac{v_n}{v^n_0}\right)^{\delta_n} - \left(\frac{s^*(v_n, \Delta v_n)}{s_n}\right)^2\right] \tag{4}$$

$$s^*(v_n,\ \Delta v_n) = s^n_0 + T_n v_n + \frac{v_n \Delta v_n}{2\sqrt{\bar{a}_n \bar{b}_n}} \tag{5}$$

where
a^n_{IDM} = acceleration,
s_n = actual gap,
s^* = desired minimum gap,
v_n = velocity, and
Δv_n = velocity difference for vehicle n.

Free acceleration exponent, δ_n, the desired time gap, T_n, jam distance, s^n_0, maximum acceleration, $\bar{a}_n$, desired deceleration, $\bar{b}_n$, and desired velocity, v^n_0, are parameters for vehicle n. The improved CV models, which consider the impacts of driver compliance or communication topology between vehicles (*32–35*), are not included in this paper because our focus is on the impact of CACC vehicles on traffic stability. Future studies could consider these improvements and use real-world CV data to calibrate model parameters to simulate more realistic cases.

Autonomous Vehicles

By capturing other drivers' behavior via the on-board sensors, AVs are assumed to have the capability of reacting almost instantaneously to any changes in the driving environment. We adopted Talebpour and Mahmassani's (*6*) modified microscopic traffic simulation model, MIXIC, based on research by Van Arem et al. (*36*). This model considers sensor characteristics in the modeling process and assumes that all AVs are equipped with similar sensors. It is also reasonable to assume that the speed of the AVs should be low enough to allow them to stop within the sensor detection range because AVs only can observe vehicles within their sensors' detection range. Desired acceleration, considering safety constraints, is calculated as

$$\begin{aligned} a^d_n(t) = {} & k_a \cdot a_{n-1}(t-\tau) + k_v \cdot (v_{n-1}(t-\tau) - v_n(t-\tau)) \\ & + k_s \cdot (s_n(t-\tau) - s_{ref}) \end{aligned} \tag{6}$$

where
n and $n-1$ represent the AV and its preceding vehicle,
a^d_n is the desired acceleration of vehicle n,
τ is the reaction time of the vehicle,
k_a, k_v, and k_s are parameters,
s_n is the spacing obtained by the sensor,
s_{ref} is the maximum among safe following distances (s_{safe}), which is based on the reaction time τ (s_{system}), and minimum distance (s_{min} = 2 m in this paper).

$$s_{ref} = \max\{s_{safe},\ s_{system}, s_{min}\} \tag{7}$$

$$s_{safe} = \frac{v^2_{n-1}}{2}\left(\frac{1}{a^{decc}_n} - \frac{1}{a^{decc}_{n-1}}\right) \tag{8}$$

$$s_{system} = v_n \tau \tag{9}$$

where
v_n = speed of vehicle n,
v_{n-1} = speed of preceding vehicle, and
a^{decc}_n = maximum deceleration of vehicle n.

The maximum safe speed is calculated to consider the maximum possible deceleration for the AVs as follows:

$$\Delta x_n = (x_{n-1} - x_n - l_{n-1}) + v_n \tau + \frac{v^2_{n-1}}{2a^{decc}_{n-1}} \tag{10}$$

$$\Delta x = \min\{Sensor\ detection\ range, \Delta x_n\} \tag{11}$$

$$v_{max} = \sqrt{-2a^{decc}_n \Delta x} \tag{12}$$

where
x_n = position of vehicle n,
l_n = length of vehicle n,
Δx = distance within the sensor detection range, and
v_{max} = maximum safe speed.

Finally, the acceleration of the AVs can be calculated as

$$a_n(t) = \min\{a^d_n(t),\ k(v_{max} - v_n(t))\} \tag{13}$$

where k is a parameter.

Connected and Automated Vehicles Under Cooperative and Adaptive Cruise Control

CAVs are considered to interact with other CVs and infrastructure via sharing information, receiving information, or both, and reacting instantly to any changes. Based on the characteristic of CAVs for cooperative

driving automation, we selected the CACC model by Milanés and Shladover (*26*) as follows:

$$e_n = x_{n-1} - x_n - t_h v_n \tag{14}$$

$$v_n = v_{n_{prev}} + k_p e_n + k_d \dot{e}_n \tag{15}$$

where
e_n and $\dot{e}_n$ are the spacing error and its first derivative of vehicle n,
x_n and x_{n-1} are the current positions of vehicle n and its preceding vehicle,
t_h is the constant time headway,
v_n and $v_{n_{prev}}$ are the speed in the current and previous time of vehicle n,
k_p is the control parameter of spacing error of vehicle n, and
k_d is the control parameter of the first derivative of spacing error (i.e., speed error) of vehicle n.

Stability Analysis for Homogeneous CAV Traffic Flow

To understand the stability of the selected CACC model for CAV cooperative driving automation, we derived the stability conditions under homogeneous CAV traffic flow. The stability conditions provide a theoretical criterion with which to set control parameters for the CACC model to guarantee stability.

Stability Conditions

To find the stability conditions, we used the spacing $s_n = x_{n-1} - x_n$ to rewrite the model in Equations 14 and 15 as in Equations 16 and 17,

$$e_n = s_n - t_h v_n \tag{16}$$

$$v_n = v_{n_{prev}} + k_p(s_n - t_h v_n) + k_d(\dot{s}_n - t_h \dot{v}_n) \tag{17}$$

where $\dot{s}_n = \Delta v$ is the speed difference. In addition, there is a relationship between v_n and $v_{n_{prev}}$ based on the velocity formula $v_n = v_{n_{prev}} + \dot{v}_n \Delta t$, where Δt is the control time interval. The acceleration of vehicle n can then be described as

$$a_n = \dot{v}_n = \frac{k_p s_n - k_p t_h v_n + k_d \Delta v}{k_d t_h + \Delta t} \tag{18}$$

Thus, it is easy to identify that the acceleration can be written as the function of spacing, speed, and speed difference:

$$a_n = \frac{k_p}{k_d t_h + \Delta t} s_n + \frac{k_d}{k_d t_h + \Delta t} \Delta v + \frac{-k_p t_h}{k_d t_h + \Delta t} v_n \tag{19}$$

Substitute $f_s^{CAV} = \frac{k_p}{k_d t_h + \Delta t}$, $f_{\Delta v}^{CAV} = \frac{k_d}{k_d t_h + \Delta t}$ and $f_v^{CAV} = \frac{-k_p t_h}{k_d t_h + \Delta t}$ into Equation 19 to give

$$a_n = f_s^{CAV} s_n + f_{\Delta v}^{CAV} v_{n-1} + (f_v^{CAV} - f_{\Delta v}^{CAV}) v_n \tag{20}$$

where the derivative of spacing $\dot{s}_n = v_{n-1} - v_n = \Delta v$.

Following the review of stability conditions for car-following models in the study by Sun et al. (*14*), we applied the direct transfer function method to analyze stability in Proposition 1. The basic idea of the approach is to focus on the frequency response between the input and output of a system, which means considering two consecutive vehicles as a system by which to view perturbation propagation (*37*).

Proposition 1. For any feasible control parameter, k_d, Milanés and Shladover's (*26*) CACC model is string stable if Equation 21 is held,

$$k_p > \frac{2\Delta t}{t_h^2} \tag{21}$$

where
k_p = control parameter,
Δt = control time interval, and
t_h = constant time headway.

Proof. We used the transfer function, $G(i\omega)$, between the input and the output of a system to find the string stability criterion. Note that we assumed the perturbation of the leading vehicle was a steady oscillation, $v_0(t) = e^{i\omega t}$, and then $v_n(t) = G^n(i\omega)e^{i\omega t}$ ($i\omega$ is commonly used in control theory to initialize a steady signal in the frequency domain).

First, based on this assumption, we can ascertain that

$$G(i\omega) = \frac{f_s + i\omega f_{\Delta v}}{f_s - \omega^2 - i\omega(f_v - f_{\Delta v})} \tag{22}$$

It is easy to show that the perturbation in the traffic stream will not be amplified to the upstream traffic if

$$\|G(i\omega)\|_\infty = \frac{\sqrt{f_s^2 + \omega^2 f_{\Delta v}^2}}{\sqrt{(f_s - \omega^2)^2 + \omega^2 (f_v - f_{\Delta v})^2}} < 1 \tag{23}$$

Then,

$$2f_s - f_v^2 + 2f_v f_{\Delta v} < \omega^2 \tag{24}$$

We assumed $\omega \to 0$ would place the strongest constraint on the inequality, which also implies long-wavelength instability occurs first. Thus, from Equation 24, the string stability criterion is calculated as

$$\frac{f_v^2}{2} - f_s - f_v f_{\Delta v} > 0 \geqslant -\omega^2 \tag{25}$$

Substitute $f_s = \frac{k_p}{k_d t_h + \Delta t}$, $f_{\Delta v} = \frac{k_d}{k_d t_h + \Delta t}$ and $f_v = \frac{-k_p t_h}{k_d t_h + \Delta t}$, which can be obtained from Equation 19:

$$\frac{1}{2}\left(\frac{-k_p t_h}{k_d t_h + \Delta t}\right)^2 - \frac{k_p}{k_d t_h + \Delta t} - \frac{-k_d}{k_d t_h + \Delta t}\frac{k_p t_h}{k_d t_h + \Delta t} > 0 \tag{26}$$

In this case, we found the relationship among control parameter k_p, control time interval Δt, and constant time headway t_h to gurantee stable traffic. The stability condition is described as

$$k_p > \frac{2\Delta t}{t_h^2} \tag{27}$$

Therefore, k_p should be larger than $2\Delta t/t_h^2$ to achieve string stability in a homogeneous CAV environment.

Based on the stability conditions in Proposition 1, the following sections focus on the boundary condition of the traffic state among three factors: the control parameter, k_p; the constant time headway, t_h; and the control time interval, Δt.

The Minimum Constant Time Headway to Guarantee String Stability

In this section, we will discuss how the minimum constant time headway, t_h^{min}, can affect string stability. According to Equation 27, the perturbation will damp rather than amplify if the product of the control parameter, k_p, and the constant time headway, t_h, is greater than $2\Delta t$. In general, the time interval, Δt, is set as the constant value with some physical limitations of the vehicle and communication systems. One example is shown in Figure 1, which indicates the state relationship between k_p and t_h. Under a scenario of 0.01 s control time interval setting, the frontier line of the boundary conditions for guaranteeing stability shows that t_h^{min} gradually decreases when k_p increases from 0.1 to 0.9. For $k_p = 0.1$, t_h^{min} is near 0.45 s; in contrast t_h^{min} is about 0.15 s for $k_p = 0.9$. This result indicates that a greater k_p needs a shorter t_h to guarantee a stable traffic state. In other words, if t_h is set as greater than 0.45 s, all possible values of k_p located between 0.1 and 0.9 could be selected to achieve string stability.

The Impact of the Length of the Control Time Interval on String Stability

As in Proposition 1, the length of the control time interval, Δt, also influenced string stability. To reveal the relationship between k_p and its corresponding minimum constant time headway, t_h^{min}, under different lengths of control time interval settings, Figure 2 shows the trends among $\Delta t = 0.01,\ 0.02,\ 0.05$, and 0.1 s. In each case, the results were consistent with the finding relating to the inversely increasing relationship between k_p and t_h^{min} (i.e., t_h^{min} decreases while k_p increases). Moreover, the shorter control time interval setting led to a shorter t_h. For example, for $k_p = 0.3$, t_h^{min} was about 0.25 s, 0.35 s, 0.6 s, and

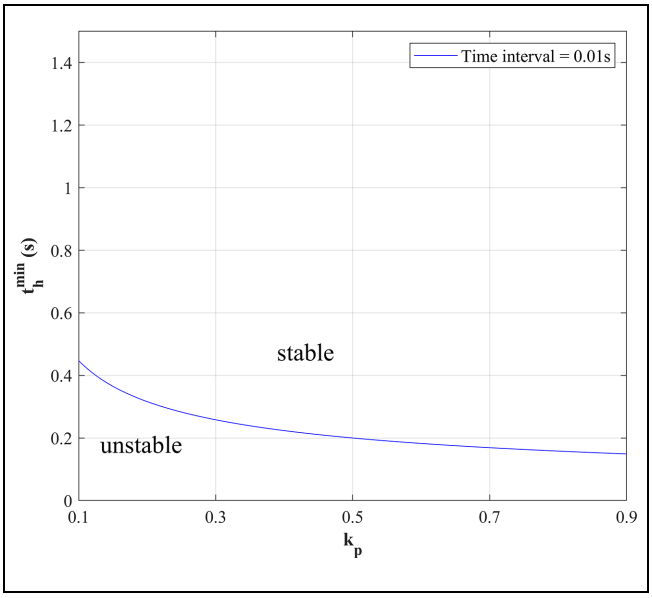

Figure 1. Stability conditions of parameter k_p and minimum constant time headway t_h^{min}.

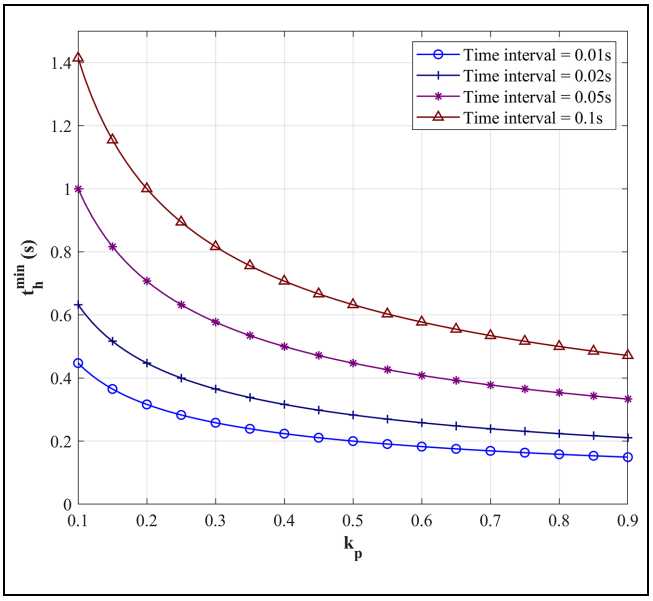

Figure 2. Stability conditions of k_p and t_h^{min} under different control time intervals.

0.8 s, which corresponded to $\Delta t = 0.01$ s, 0.02 s, 0.05 s, and 0.1 s, respectively. It was clear that $\Delta t = 0.01$ s could guarantee string stability with the shortest minimum constant time headway, t_h^{min}.

Therefore, to guarantee stable traffic flow, we found there was a minimum constant time headway for each control parameter and time interval setting. The stability conditions provided a theoretical criterion with which to select control parameters for the selected CACC controller under homogenous CAV traffic.

Stability Analysis for Heterogeneous Traffic Flow

The stability conditions of the CACC controller under homogeneous CAV traffic in the previous section revealed the criterion with which to select parameter values to guarantee string stability. This section analyzes the impact of the cooperative driving automation of the CACC controller under heterogeneous traffic flow mixed with HDVs, CVs, and AVs.

Stability Function and Definitions

In general, the acceleration function, a_n, represents the driver's response in a time-continuous model in relation to the spacing, s_n, the speed difference , Δv_n, to the preceding vehicle, and the driver's speed , v_n. Thus, a car-following model could be simply formulated as follows (*39*):

$$\dot{x}_n = v_n \tag{28}$$

$$\dot{v}_n = f(s,\ \Delta v, v) \tag{29}$$

As indicated previously, string stability is a significant constraint to ensuring perturbations will not be amplified to upstream traffic. Considering small perturbations in headway and equilibrium speed of a vehicle in a platoon of infinite length and linearizing Equations 28 and 29, Ward (*5*) presented a simple formula for a heterogeneous traffic flow to calculate the stability condition. It implies that the perturbation in the traffic stream will not be amplified to the upstream traffic in this condition. Therefore, the traffic flow is regarded as being stable when the following stability function is positive:

$$\sum_n \left[\frac{f_v^{n^2}}{2} - f_{\Delta v}^n f_v^n - f_s^n\right]\left[\prod_{m\neq n} f_s^m\right] > 0 \tag{30}$$

where n denotes the vehicle types and $f_s^n = \frac{\partial f(s,\ \Delta v, v)}{\partial s}$, $f_{\Delta v}^n = \frac{\partial f(s,\ \Delta v, v)}{\partial \Delta v}$, and $f_v^n = \frac{\partial f(s,\ \Delta v, v)}{\partial v}$ are the partial derivatives of the spacing, speed difference, and speed, respectively. Following Equation 30, this section explores the stable regime and the influence of CAVs in mixed traffic flow composed of HDVs, CVs, AVs, and CAVs.

Definitions. To clearly describe and compare various traffic conditions, the following definitions were used in this study. Figure 3 illustrates these definitions graphically.

Definition 1. Free-flow speed, v_f. The average speed of vehicles over an urban street segment without signalized intersections, or over a basic freeway or multilane highway segment, under conditions of low volume. (HCM 2000, (*38*))

In this paper, the free-flow speed v_f is set as the speed limit 30 m/s (= 67.1 mph).

Definition 2. Equilibrium speed, v_e. A speed at which traffic flow is in complete equilibrium and platoon perturbations do not tend to amplify to upstream traffic.

From empirical observations, there exists an equilibrium spacing s^* and equilibrium speed v_e so that $f(s^*,\ 0, v_e) = 0$ (*30*).

Definition 3. String stable. Traffic flow is string stable if local perturbations dissipate everywhere, even in arbitrarily long vehicle platoons (*39*).

Based on work by Ward (*5*), when all calculated values of the stability function (Equation 30) at any equilibrium speed ($v_e \leqslant v_f$) are greater than 0 (i.e., stable), the current traffic condition is defined as string stable. Figure 3 shows the string stable line (blue line), which is above 0 for the equilibrium speed from 0 to free-flow speed.

Definition 4. Partially stable. In contrast to string stable, the partially stable condition means that the values of the stability function (Equation 30) are not

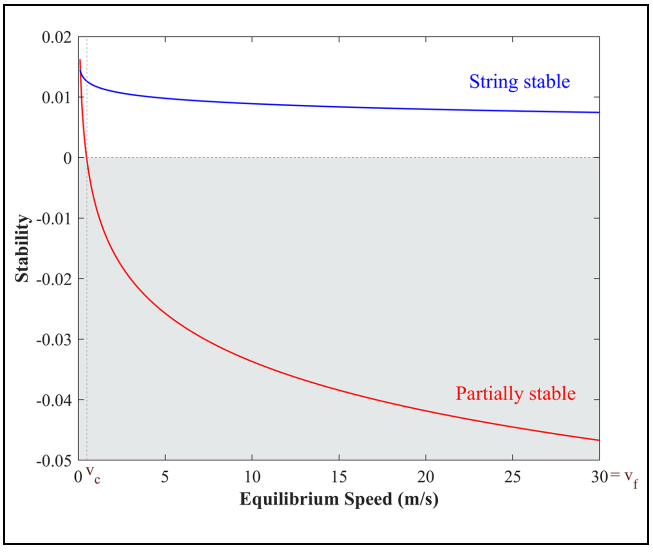

Figure 3. Stability conditions.

always greater than 0 and become negative (i.e., unstable) at certain equilibrium speeds.
Figure 3 shows an example of a partially stable condition (red line) that crosses the 0 line for equilibrium speed from 0 to free-flow speed.
Definition 5. Critical speed, v_c. The speed threshold at which traffic becomes unstable.

With the expansion of the above definitions, this study followed the definition of critical speed, v_c, used by Talebpour and Mahmassani (*6*) to define the speed threshold at which traffic becomes unstable. In other words, the stability function value firstly becomes negative at the critical speed, where the critical speed in a string stable traffic condition is larger than v_f and therefore defined as v_f in this paper. Figure 3 shows the critical speed, v_c, for the partially stable line, where $0 \leqslant v_c \leqslant v_f$. Since the stability function never becomes negative or v_c is greater than v_f for a string stable line, we defined $v_c \geqslant v_f$ under the string stable condition.

Acceleration Function Derivatives. To determine the stability condition in Equation 30 (*5*), we derive the acceleration function derivatives for HDVs, CVs, AVs, and CAVs in this subsection.

Acceleration Derivatives for Human-Driven Vehicles. This study used the PT-based acceleration model by Hamdar et al. (*27*) to model HDVs. This model calculates the prospect index to determine the driver's behavior choice. Adopting the Wiener process, Talebpour and Mahmassani (*6*) calculated the partial derivatives as in Equations 31 to 33:

$$f_s^{HDV} = \frac{2}{\tau_{max}^2} \tag{31}$$

$$f_{\Delta v}^{HDV} = \frac{-2}{\tau_{max}} \tag{32}$$

$$f_v^{HDV} = \frac{2\alpha}{\tau_{max}} \sqrt{2\ln\left(\frac{w_c \tau_{max}}{2\sqrt{2\pi}\alpha v_e}\right)} + \frac{2\alpha v_e}{\tau_{max}} \left[\frac{1}{\sqrt{2} v_e} \left(\ln\left(\frac{w_c \tau_{max}}{2\sqrt{2\pi}\alpha v_e}\right)\right)^{-\frac{1}{2}}\right] \tag{33}$$

where
velocity uncertainty variation coefficient $\alpha = 0.08$,
weighing factor for accidents $w_c = 10000.0$, and
maximum anticipation time horizon $\tau_{max} = 4.0$ s.

Acceleration Derivatives for Connected Vehicles. In the case of CVs, the partial derivatives of the IDM are described in Equations 34 to 36:

$$f_s^{CV} = \frac{2\bar{a}}{s} \left(\frac{s_0 + Tv_e}{s}\right)^2 \tag{34}$$

$$f_{\Delta v}^{CV} = -\frac{v_e}{s^2} \sqrt{\frac{\bar{a}}{\bar{b}}} (s_0 + Tv_e) \tag{35}$$

$$f_v^{CV} = -\frac{\bar{a}\delta}{v_0} \left(\frac{v_e}{v_0}\right)^{\delta - 1} - \frac{2\bar{a}T}{s^2}(s_0 + Tv_e) \tag{36}$$

where
$\delta = 4.0$,
$T = 2.0$ s,
$\bar{a} = 4.0$ m/s^2,
$\bar{b} = 2.0$ m/s^2, and
$s_0 = 2.0$ m are used in this paper.

Acceleration Derivatives for Autonomous Vehicles. Based on Talebpour and Mahmassani (*6*), we assumed that the acceleration of the leader would be 0 during the estimation time. Thus, the partial derivatives are constant as in Equations 37 to 39:

$$f_s^{AV} = k_s \tag{37}$$

$$f_{\Delta v}^{AV} = k_v \tag{38}$$

$$f_v^{AV} = -k_s \tau \tag{39}$$

This study used $\tau = 2.0$ s, $k = 1.0$, $k_a = 1.0$, $k_v = 0.58$, and $k_s = 0.1$ (*36*).

Acceleration Derivatives for Connected and Automated Vehicles With CACC Controllers. In the previous section, we derived the acceleration model (Equation 19) of Milanés and Shladover's (*26*) CACC controller in relation to spacing, speed, and speed difference. Then, the partial derivatives can be easily calculated as in Equations 40 to 42:

$$f_s^{CAV} = \frac{k_p}{k_d t_h + \Delta t} \tag{40}$$

$$f_{\Delta v}^{CAV} = \frac{k_d}{k_d t_h + \Delta t} \tag{41}$$

$$f_v^{CAV} = \frac{-k_p t_h}{k_d t_h + \Delta t} \tag{42}$$

Stability Analysis for Mixed HDV and CAV Traffic Flow

The driving environment consisting of HDVs and CAVs (under CACC) is analyzed in this subsection. We focus on the stability conditions and the corresponding impacts of different parameter designs in the CACC model, especially the relationship among parameter k_p, the constant time headway, t_h, and the length of control time interval, Δt. Then, we select the appropriate parameter values and compare the stability with other vehicle types.

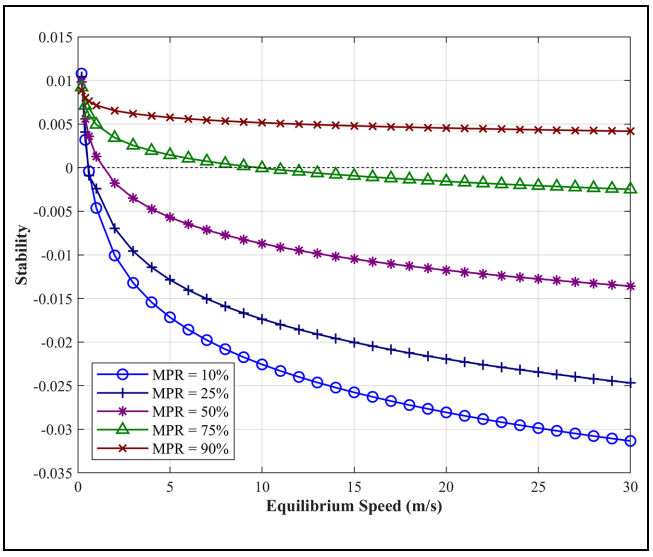

Figure 4. Stability analysis of mixed human-driven vehicles (HDVs) and connected and automated vehicles (CAVs) with experimental parameter values.
Note: MPR = market penetration rate.

Stability Conditions for Mixed HDVs and CAVs. Considering the different compositions of traffic flows, we analyzed the stability for different MPRs of each kind of vehicle type. Following Equation 30 presented by Ward (*5*), the stability condition for mixed HDVs and CAVs can be written in Equation 43:

$$P_{HDV}\left(f_s^{CAV}\right)\left(\frac{f_v^{HDV^2}}{2}-f_{\Delta v}^{HDV}f_v^{HDV}-f_s^{HDV}\right) + P_{CAV}\left(f_s^{HDV}\right)\left(\frac{f_v^{CAV^2}}{2}-f_{\Delta v}^{CAV}f_v^{CAV}-f_s^{CAV}\right)>0 \quad (43)$$

where P_{HDV} and P_{CAV} denote the MPR of HDVs and CAVs, respectively. Figure 4 shows the stability analysis results of different MPRs of CAVs, where the model parameters were assigned as in Milanés and Shladover (*26*): $k_p = 0.45$, $k_d = 0.25$, $t_h = 1.1\ s$, and $\Delta t = 0.1\ s$. This figure reveals that a higher CAV MPR improved the stability of traffic flow and even guaranteed string stability for all speeds from 0 m/s to 30 m/s (this study set it as the free-flow speed) under the situation of 90% CAVs.

The Impact of CAV Control Parameters (k_p and t_h) on String Stability. To further explore the influence of parameter selection on the CACC controller in heterogeneous traffic flow, this section studies the relationship between stability and constant time headway, t_h, for a given control time interval (e.g., 0.1 s) as the stability condition in Proposition 1. From the previous discussion, the stability condition was derived to determine the speed threshold (i.e., critical speed) of instability. Thus, the critical speed can be described as

$$v_c = \mathcal{V}(k_p,\ t_h,\ \Delta t) \quad (44)$$

where $\mathcal{V}$ is the function of the control parameter, k_p, constant time headway, t_h, and control time interval, Δt. Furthermore, based on Equation 44 and using Figure 5*d* as an example to illustrate the relationship, two indicators, v_c^{min} and v_c^{max}, can be defined as follows:

Definition 6. Minimum critical speed, $\boldsymbol{v_c^{min}}$. Given the MPR of each vehicle type and control time interval, for all control parameters, k_p, and constant time headway, t_h, across from their corresponding lower bounds and upper bounds, v_c^{min} is the minimum of all critical speeds,

$$v_c^{min} = \min\{v_c\},\ \forall k_p \in [L_{k_p},\ U_{k_p}], t_h \in [L_{t_h},\ U_{t_h}] \quad (45)$$

where L_{k_p} and L_{t_h} are the lower bounds of k_p and t_h, and U_{k_p} and U_{t_h} are the upper bounds of k_p and t_h. For example, as shown in Figure 5*d*, v_c^{min} is the minimum critical speed 0.3 m/s (marked in red), where $L_{k_p} = 0.35$, $U_{k_p} = 0.55$, $L_{t_h} = 0.6$ s, and $U_{t_h} = 3.0$ s.

Definition 7. Maximum critical speed, $\boldsymbol{v_c^{max}}$. Given the MPR of each vehicle type and control time interval, for all control parameters, k_p, and constant time headway, t_h, across from their corresponding lower bounds and upper bounds, v_c^{max} equals free-flow speed, v_f, if there exists a critical speed greater than v_f (i.e., string stable condition defined in Definition 5). Otherwise, v_c^{max} is the maximum of all critical speeds.

$$v_c^{max} = \begin{cases} v_f,\ if\ \exists\ v_c > v_f \\ \max\{v_c\},\ \forall\ v_c \leqslant v_f \end{cases},\ \forall k_p \in [L_{k_p},\ U_{k_p}], t_h \in [L_{t_h},\ U_{t_h}] \quad (46)$$

where L_{k_p} and L_{t_h} are the lower bounds of k_p and t_h, and U_{k_p} and U_{t_h} are the upper bounds of k_p and t_h. In Figure 5*d*, $v_c^{max} = 30\ m/s = v_f$ (marked in dark blue), where $L_{k_p} = 0.35$, $U_{k_p} = 0.55$, $L_{t_h} = 0.6$ s, and $U_{t_h} = 3.0$ s.

Thus, with the characteristic of critical speed, three cases of stability regions by selecting k_p and t_h can be described as follows:

Case 1. Absolutely Stable Region. The absolutely stable region is defined at $v < v_c^{min}$, and then any selection of k_p and t_h can reach string stable at this speed level. In addition,

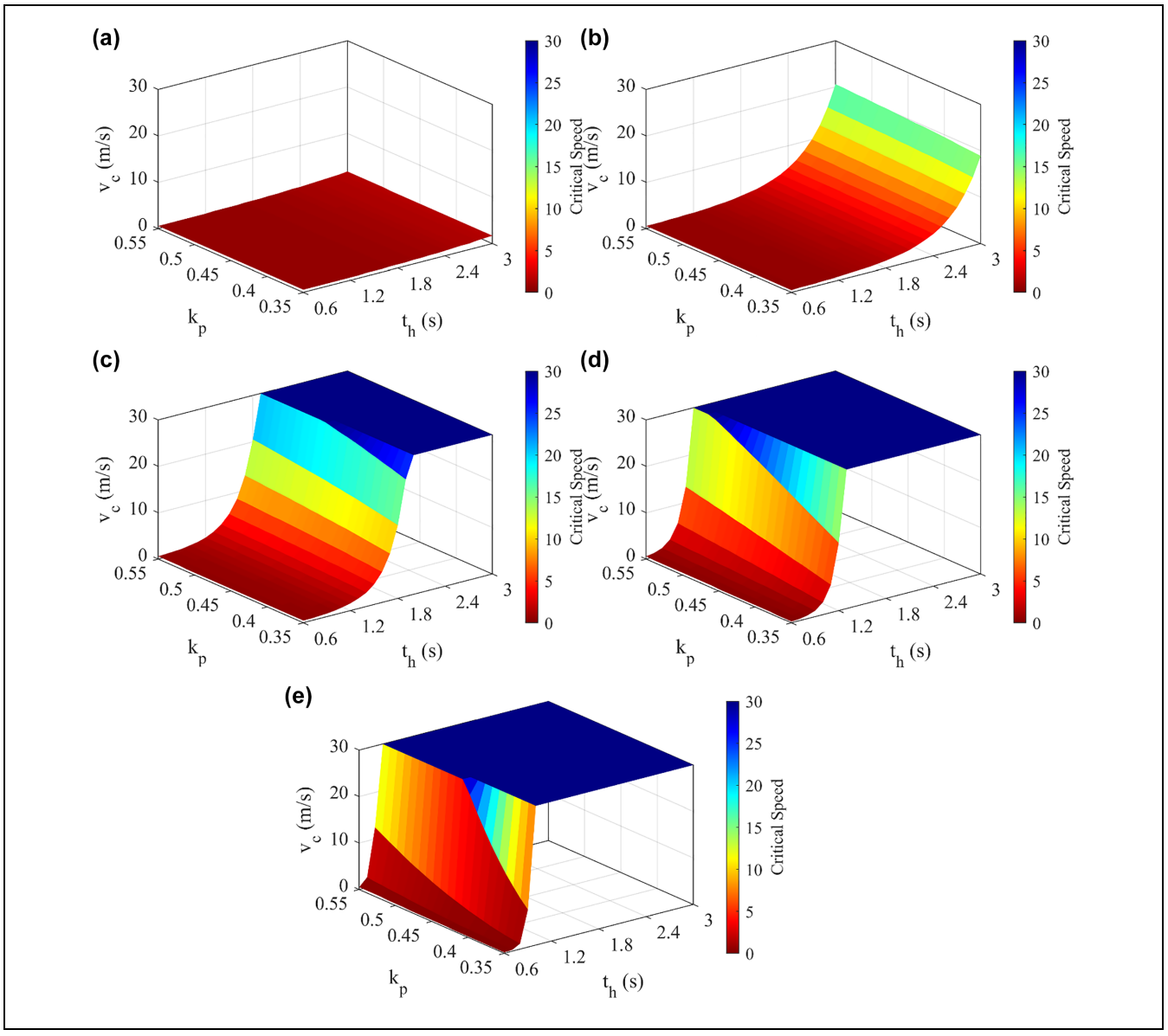

Figure 5. Critical speed analysis of different k_p and t_h with $\Delta t = 0.1$ s: (*a*) 10% connected and automated vehicle (CAV), (*b*) 25% CAV, (*c*) 50% CAV, (*d*) 75% CAV, and (e) 90% CAV.

$v_c^{min} = v_c^{max} = v_f$ also means the absolutely stable region happens at any speed (less than free-flow speed).

Case 2. Conditionally Stable Region. The conditionally stable region is defined at $v_c^{min} \leqslant v \leqslant v_c^{max}$. At this speed level, parts of the selection of k_p and t_h can reach string stable and the other parts of selection of k_p and t_h result in unstable traffic.

Case 3. Absolutely Unstable Region. The absolutely unstable region is defined at $v > v_c^{max} \neq v_f$. With the current speed level, all possible selections of k_p and t_h lead to unstable traffic flow.

For example, as shown in Figure 5*d*, the corresponding critical speed, v_c, of each selection of k_p and t_h with 75% MPR of CAV, $v_c^{min} = 0.3\ m/s$, and $v_c^{max} = v_f = 30\ m/s$. It is clear from this figure that the critical speed grows when t_h also increases. On the other hand, the trend for a larger k_p leading to a higher v_c at the same t_h is also revealed in Figure 5*d*, via the gradually changing color, which implies the larger k_p produces better stability.

In addition, the plane shape of the critical speed at 30 m/s presents the feasible selections to remain string stable in the mixed traffic flow. Namely, the larger area of the plane implies more stable selections of k_p and t_h to choose from. Therefore, the ideal condition would be the entire

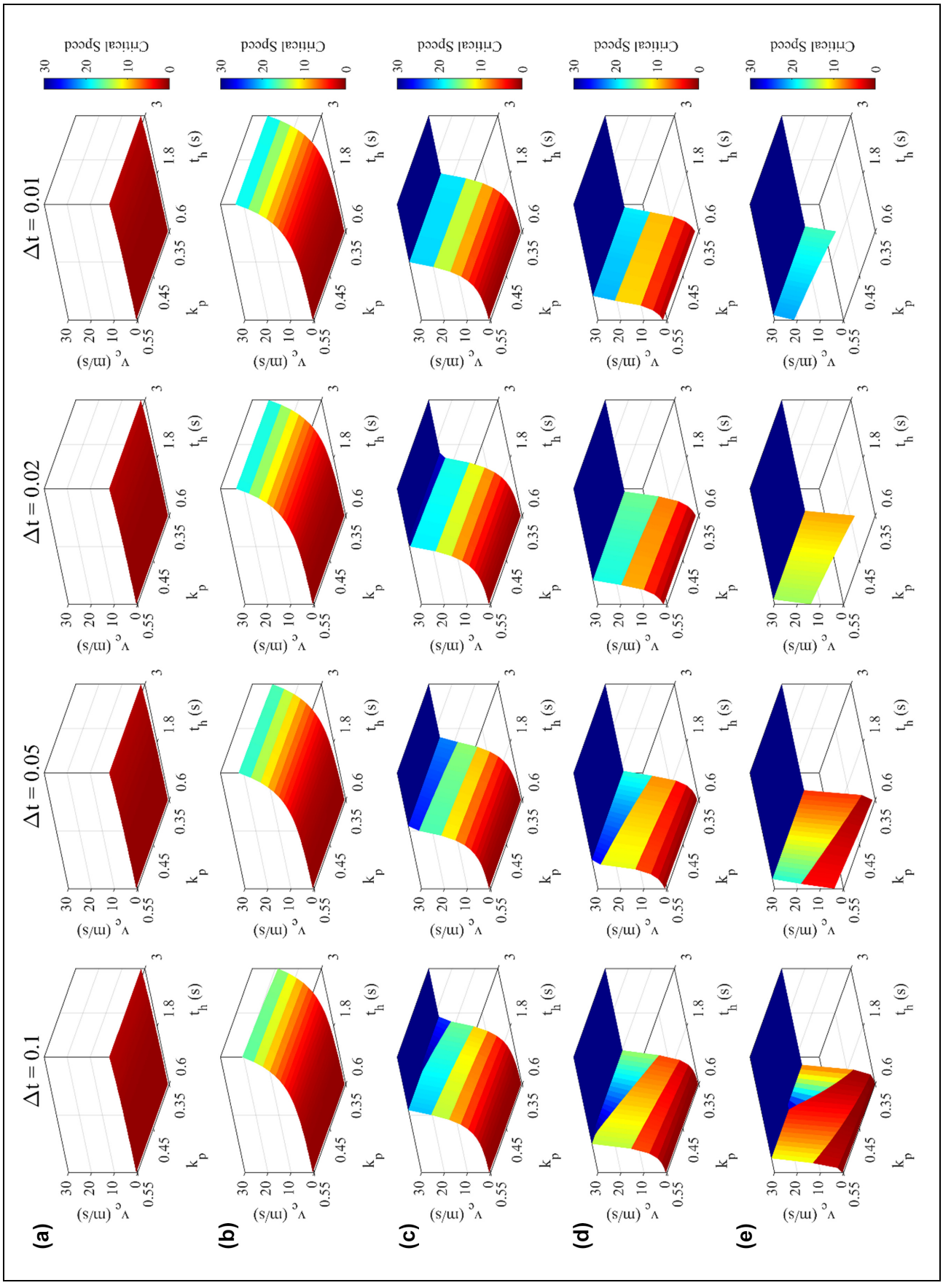

Figure 6. Critical speed analysis of different k_p and t_h with different Δt: (*a*) 10%, (*b*) 25%, (*c*) 50%, (*d*) 75%, and (*e*) 90%.

plane at v_f so that any selection of parameters will not affect the stability (i.e., $v_c^{min} = v_c^{max} = v_f$), that is, the largest absolutely stable region.

However, Figure 5*a* indicates the opposite of the ideal condition. As the CAV MPR is 10%, the difference between v_c^{min} and v_c^{max} is not clear. Both of them are less than 20 m/s and the whole figure looks like a plane at a low speed level. This result also implies that no matter how large t_h is, the CAV cannot maintain stability as well as in Figure 5*d* with the low (10%) MPR.

Figure 5, *a* to *e* , show the relationship between critical speed, k_p, and t_h under 10%, 25%, 50%, 75%, and 90% CAV, respectively. Based on the above analysis, the larger area at v_f presents greater parameter choices that will ensure string stability of the traffic flow. Comparing the five scenarios, the 90% CAV scenario has the most selections with $v_c = v_f$. String stable selections are only evident in Figure 5, *c* to *e* (the others are partially stable selections), which means that CAV has string stability at a higher MPR. Also, comparing these three figures, the critical speed of all selections at 90% CAV grows quickly when t_h increases. In other words, it has the selection with the shortest t_h in this case.

The Impact of the Length of the Control Time Interval on String Stability. The examples in the above subsection used 0.1 s as the control time interval for stability analysis. This subsection studies the impact of the length of the control time interval on string stability. Figure 6 indicates Δt = 0.1 s, 0.05 s, 0.02 s, and 0.01 s under different CAV MPRs. Among several scenarios, high CAV MPRs (e.g., 75%) illustrate the trend. For example, Figure 6 Row *d* presents the relationship among k_p, t_h, and critical speed, v_c, with different time intervals under 75% CAV. Then, observing from Column 1 to Column 4 in Row *d*, v_c gradually increases. Similar observations can be found in Rows *c* and *e*. This indicates that the smaller the length of the control time interval, meaning a higher frequent controller, the better the traffic stability in these cases.

Conversely, the cases of low CAV MPR do not have such an obvious change among the different time interval settings. In Figure 6 Rows *a* and *b*, the patterns are similar under different Δt. In other words, the influences of k_p and t_h on v_c in the low CAV MPR cases are not as significant as those in the high MPR of CAV cases.

Summarizing the above discussion, the selection of Δt did not clearly affect critical speed, which implies the capacity to maintain string stability in 10% and 25% CAV cases. In contrast, the smaller Δt obviously enhanced the stability with higher critical speeds in 50%, 75%, and 90% CAV cases.

CACC Control Parameter Selection Based on Stability Analysis. From the above discussion, there is a minimum constant time headway required for every control parameter selection, k_p, under different control time interval settings. From the previous finding and observations, this section adopts parameter values composed of $k_p = 0.55$, $k_d = 0.25$, the minimum time headway 1.8 s, and a control time interval of 0.01 s to test the stability conditions among different MPRs of CACC traffic flow.

Compared with Figure 4 that uses parameter values from literature (*26*), the improvement in stability on all MPRs of CAV in Figure 7 is obvious. In addition to 90% MPR in Figure 4, 50%, 75%, and 90% MPR in Figure 7 show the capacity to guarantee string stability at any equilibrium speed (i.e., $v_c \geqslant v_f$). Also, the critical speeds of 10% and 25% MPR in Figure 7 are higher than those in Figure 4. Therefore, based on this comparison, these parameter values were used for further analysis.

Comparison of Mixed HDVs and CVs, and Mixed HDVs and AVs. This section tests the performance of the current CAV (under CACC) with other vehicle types. Figure 8 compares the stability of the same MPRs of CAVs, CVs, and AVs under different MPRs of HDVs. As shown in Figure 8, *a* and *b*, under high HDV levels, 10% AV and 25% AV perform better than the other two types of vehicles and guarantee stability, which is greater but near 0. In contrast, CVs and CAVs are partially stable in these two cases.

Under low HDV levels, CAV clearly improves stability performance in Figure 8, *c* to *e*. Although CV has a higher stability function value in the beginning, it quickly

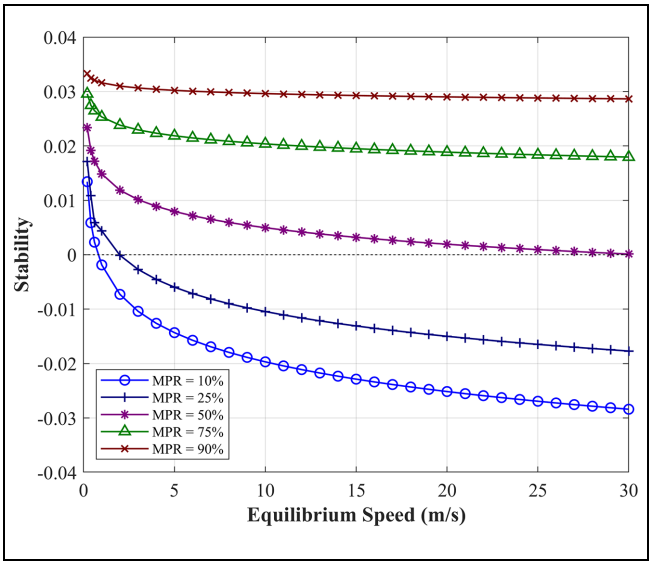

Figure 7. Stability analysis of mixed human-driven vehicles (HDVs) and connected and automated vehicles (CAVs) with selected parameter values.
Note: MPR = market penetration rate.

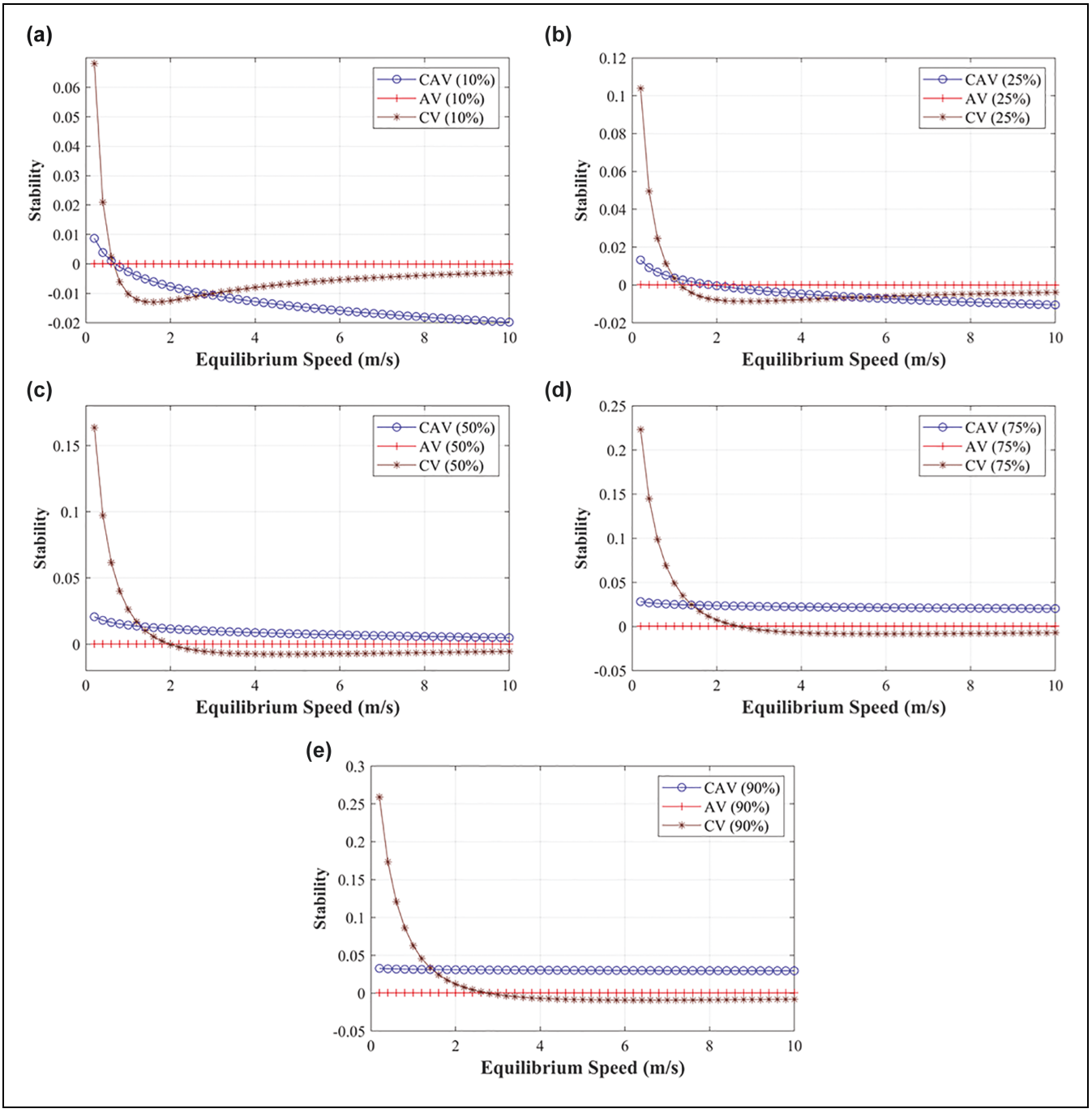

Figure 8. Stability comparisons of connected vehicles (CVs), autonomous vehicles (AVs), and connected and automated vehicles (CAVs) under different market penetration rates (MPRs): (*a*) 90% human-driven vehicle (HDV), (*b*) 75% HDV, (*c*) 50% HDV, (*d*) 25% HDV, and (*e*) 10% HDV.

drops to become negative, whereas AV and CAV are still greater than 0. Specifically, the stability of CAV maintains the string better than AVs. This trend becomes even more obvious when the HDV market penetration level decreases from 50% to 10% (i.e., 50% CAV to 90% CAV). This confirms that CAV can improve the stability in mixed traffic flow. That is to say, under low HDV situations, the higher CAV MPR has better performance on the stability than the same MPR of the CV and AV. The different spatial arrangement strategies, which may lead to different magnitudes of oscillation for the vehicles (*40*), may be investigated in future studies.

Stability Analysis for Mixed HDVs, CVs, AVs, and CACC Traffic Flow

With both connectivity and automation technologies, CAVs (with CACC controllers) can share information, receive information, or both, with other vehicles, so they are expected to have the advantage of being more stable in traffic flow. We designed scenarios composed of different MPRs of mixed HDVs, CVs, AVs, and CAVs. In addition to the MPRs of CAVs, it was also critical to test whether the amount of unconnected and unpredicted driver behavior influenced MPR levels of HDVs. Therefore, the low HDV market penetration level (25%) and high HDV market penetration level (75%) were explored. Based on Equation 30, all scenario settings and calculated critical speed values were as in Table 1.

Table 1. Designed Scenarios With Different Market Penetration Rates (MPRs)

HDV	CAV (%)	AV (%)	CV (%)	Critical speed (m/s)
High	5	10	10	2.6
HDV–MPR	10	7.5	7.5	2.4
level (75%)	15	5	5	2.3
	20	2.5	2.5	2.2
Low	15	30	30	8.8
HDV–MPR	25	25	25	9.7
level (25%)	35	20	20	11.0
	45	15	15	13.0
	55	10	10	16.1
	65	5	5	21.1

Note: CV = connected vehicle; AV = autonomous vehicle; CAV = connected and automated vehicle; HDV = human-driven vehicle.

As shown in Table 1, all critical speed values were markedly small, in the range of 2.2 m/s to 2.6 m/s, although they performed better than CV and AV cases in the previous study (*6*). As for the same 15% MPR of CAV, the critical speeds were evidently different at 8.8 m/s and 2.3 m/s under 25% and 75% HDV, respectively. This result confirmed that the performance of CAV was affected under the low MPR level. Due to the characteristic of CAV, the high percentage of HDVs strongly influenced the performance of CAV.

To extend the above discussion, we analyzed the stability function value under the lower HDV market penetration level (i.e., 25%). Figure 9, *a* and *b*, present the stability values of 15% and 25% MPR of CAV, which are both under the low HDV market penetration level. The gray colored region indicates the unstable regime, whereas the region in white represents the stable regime. Figure 9*a* shows the stability function value with a 15% CAV quickly falls to become negative, resulting in the critical speed at 8.8 m/s. In contrast, the critical speed of 25% CAV slows down to become negative at 9.7 m/s in Figure 9*b*.

To observe the impact of the penetration rates of CAV, Figure 10*a* presents the trends of stability among 15%, 25%, 35%, 45%, 55%, and 65% MPRs of CAV. The higher MPR of CAV led to a larger stable regime, which means the capability of maintaining string stability at a higher equilibrium speed. Figure 10*b* illustrates how values of critical speed positively correlate with MPRs of CAVs under low HDV market penetration levels.The

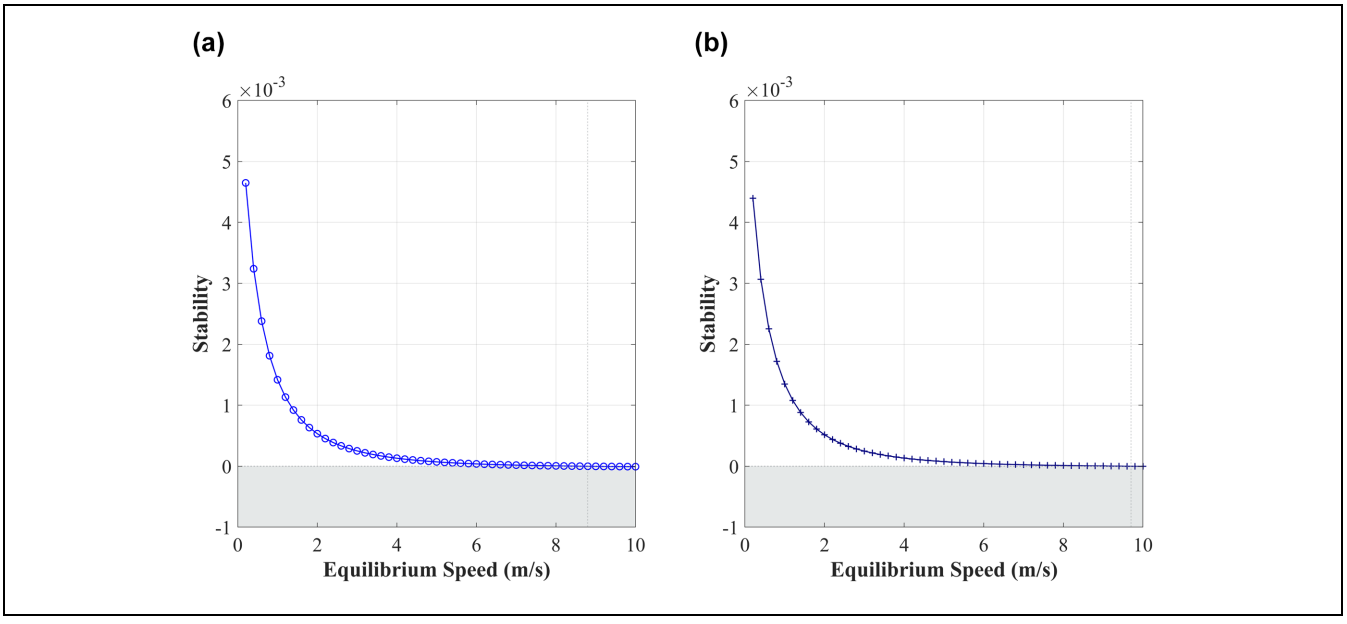

Figure 9. Stability analysis under human-driven vehicle (HDV) 25%: (*a*) connected and automated vehicle (CAV) 15% and (*b*) CAV 25%.

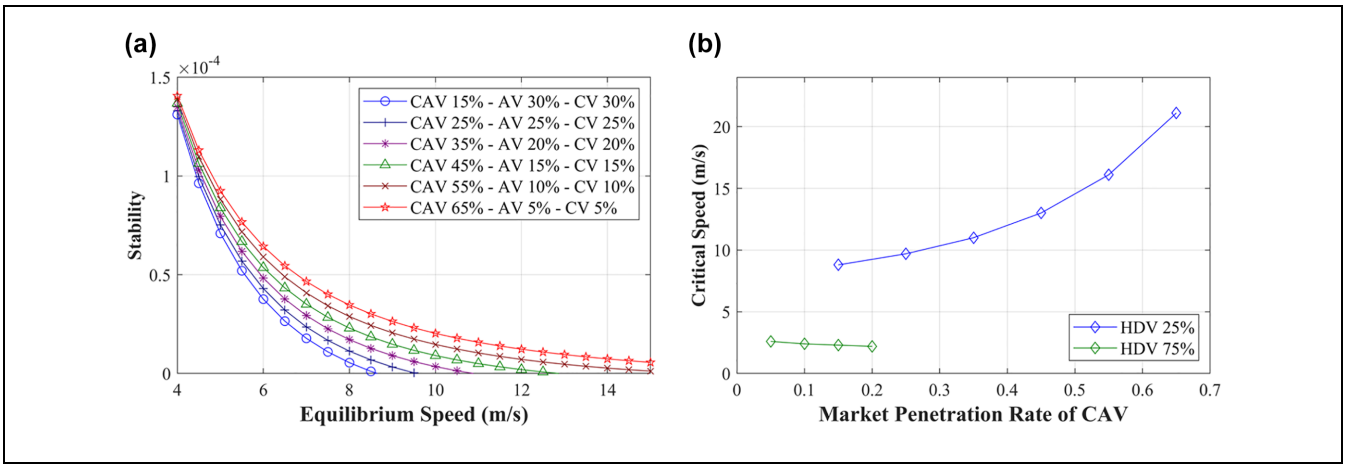

Figure 10. Stability analysis of different market penetration rates (MPRs) of CAVs: (*a*) stability under different MPRs of CAVs and (*b*) critical speed with different MPRs of CAVs.

Note: CV = connected vehicle; AV = autonomous vehicle; CAV = connected and automated vehicle; HDV = human-driven vehicle.

critical speed significantly improved from 8.8 m/s to 21.1 m/s when CAV increases the MPR from 15% to 65%. That is, CAV under CACC has the advantage of improving stability especially the higher MPRs in a mixed traffic flow.

Conclusions

In this paper, we derived the stability conditions for Milanés and Shladover's (*26*) CACC model for cooperative driving automation of CAVs and presented stability analyses for homogeneous and heterogeneous traffic. In the homogeneous CAV traffic, a minimum constant time headway with each parameter design of the CACC controller was necessary to ensure stability. The larger the control parameter and the smaller the length of the control time interval, the shorter the minimum constant time headway required to guarantee string stability. In the heterogeneous traffic with mixed HDVs and CAVs (with CACC controllers), similar to the homogeneous CAV traffic, the constant time headway and the length of the control time interval had significantly positive correlations with stability and the control parameter had a negative correlation with stability. Moreover, we also found that different MPRs of CAVs had different impacts on stability. The higher the MPRs of CAVs, such as 75% and 90%, the better their capability to ensure string stability. We also studied the impact of combined connectivity and automation technologies in CAVs on stability in heterogeneous traffic by comparing CAVs (i.e., with combined connectivity and automation technologies) with CVs (i.e., with the connectivity technology only) and AVs (i.e., with the automation technology only). From the analysis, CACC vehicles performed better than CVs and AVs with higher MPRs, which confirmed that the cooperative driving automation of CACC vehicles had the benefit of improving stability at a low MPR of HDV traffic. Communication delays, data loss issues, and lane-changing behaviors were not included in this study. For example, considering both mandatory and discretionary lane-changing behaviors can improve predictions (*41*). Future studies could be extended to relax these limitations, such as the driver compliance and communication topology, on string stability in the models.

Author Contributions

The authors confirm contribution to the paper as follows: study conception and design: Y. Hung and K. Zhang; data collection: Y. Hung and K. Zhang; analysis and interpretation of results: Y. Hung and K. Zhang; draft manuscript preparation: Y. Hung and K. Zhang. All authors reviewed the results and approved the final version of the manuscript.

Declaration of Conflicting Interests

The authors declared no potential conflicts of interest with respect to the research, authorship, and/or publication of this article.

Funding

The authors disclosed receipt of the following financial support for the research, authorship, and/or publication of this article: This research was supported by a grant from the National Science Foundation (NSF) under NSF CAREER award CMMI-1846795.

ORCID iDs

Yun-Chu Hung https://orcid.org/0000-0003-2218-670X
Kuilin Zhang https://orcid.org/0000-0002-8180-5016

References

1. Dey, K. C., L. Yan, X. Wang, Y. Wang, H. Shen, M. Chowdhury, L. Yu, C. Qiu, and V. Soundararaj. A Review of Communication, Driver Characteristics, and Controls Aspects of Cooperative Adaptive Cruise Control (CACC). *IEEE Transactions on Intelligent Transportation Systems*, Vol. 17, No. 2, 2015, pp. 491-509.
2. Wang, Z., G. Wu, and M. J. Barth. A Review on Cooperative Adaptive Cruise Control (CACC) Systems: Architectures, Controls, and Applications. *Proc., 21st International Conference on Intelligent Transportation Systems (ITSC)*, Maui, HI, IEEE, New York, November 4-7, 2018, pp. 2884-2891.
3. Peppard, L. String Stability of Relative-Motion PID Vehicle Control Systems. *IEEE Transactions on Automatic Control*, Vol. 19, No. 5, 1974, pp. 579-581.
4. Rothery, R. W. Car Following Models. *Trac Flow Theory*, 1992. https://www.fhwa.dot.gov/publications/research/operations/tft/chap4.pdf
5. Ward, J. A. *Heterogeneity, Lane-Changing and Instability in Traffic: A Mathematical Approach*. Doctoral dissertation. University of Bristol, England, 2009.
6. Talebpour, A., and H. S. Mahmassani. Influence of Connected and Autonomous Vehicles on Traffic Flow Stability and Throughput. *Transportation Research Part C: Emerging Technologies*, Vol. 71, 2016, pp. 143-163.
7. Monteil, J., M. Bouroche, and D. J. Leith. L_2 and L_∞ Stability Analysis of Heterogeneous Traffic With Application to Parameter Optimization for the Control of Automated Vehicles. *IEEE Transactions on Control Systems Technology*, Vol. 27, No. 3, 2018, pp. 934-949.
8. Wang, M. Infrastructure Assisted Adaptive Driving to Stabilise Heterogeneous Vehicle Strings. *Transportation Research Part C: Emerging Technologies*, Vol. 91, 2018, pp. 276-295.
9. Qin, W. B., and G. Orosz. Experimental Validation of String Stability for Connected Vehicles Subject to Information Delay. *IEEE Transactions on Control Systems Technology*, Vol. 28, No. 4, 2019, pp. 1203-1217.
10. Zhou, Y., and S. Ahn. Robust Local and String Stability for a Decentralized Car Following Control Strategy for Connected Automated Vehicles. *Transportation Research Part B: Methodological*, Vol. 125, 2019, pp. 175-196.
11. Zhou, Y., M. Wang, and S. Ahn. Distributed Model Predictive Control Approach for Cooperative Car-Following With Guaranteed Local and String Stability. *Transportation Research Part B: Methodological*, Vol. 128, 2019, pp. 69-86.
12. Montanino, M., and V. Punzo. On String Stability of a Mixed and Heterogeneous Traffic Flow: A Unifying Modelling Framework. *Transportation Research Part B: Methodological*, Vol. 144, 2021, pp. 133-154.
13. Wang, J., Y. Zheng, C. Chen, Q. Xu, and K. Li. Leading Cruise Control in Mixed Traffic Flow: System Modeling, Controllability, and String Stability. *arXiv Preprint arXiv:2012.04313*, 2020.
14. Sun, J., Z. Zheng, and J. Sun. Stability Analysis Methods and Their Applicability to Car-Following Models in Conventional and Connected Environments. *Transportation Research Part B: Methodological*, Vol. 109, 2018, pp. 212-237.
15. Feng, S., Y. Zhang, S. E. Li, Z. Cao, H. X. Liu, and L. Li. String Stability for Vehicular Platoon Control: Definitions and Analysis Methods. *Annual Reviews in Control*, Vol. 47, 2019, pp. 81-97.
16. Lu, X. Y., J. K. Hedrick, and M. Drew. ACC/CACC-Control Design, Stability and Robust Performance. *Proc., 2002 American Control Conference*, Vol. 6, Anchorage, AK, IEEE, New York, May 8-10, 2002, pp. 4327-4332.
17. Naus, G. J., R. P. Vugts, J. Ploeg, M. J. van De Molengraft, and M. Steinbuch. String-Stable CACC Design and Experimental Validation: A Frequency-Domain Approach. *IEEE Transactions on Vehicular Technology*, Vol. 59, No. 9, 2010, pp. 4268-4279.
18. Schakel, W. J., B. Van Arem, and B. D. Netten. Effects of Cooperative Adaptive Cruise Control on Traffic Flow Stability. *Proc., 13th International IEEE Conference on Intelligent Transportation Systems*, Funchal, Portugal, IEEE, New York, September 19-22, 2010, pp. 759-764.
19. Ploeg, J., D. P. Shukla, N. van de Wouw, and H. Nijmeijer. Controller Synthesis for String Stability of Vehicle Platoons. *IEEE Transactions on Intelligent Transportation Systems*, Vol. 15, No. 2, 2013, pp. 854-865.
20. Ngoduy, D. Instability of Cooperative Adaptive Cruise Control Traffic Flow: A Macroscopic Approach. *Communications in Nonlinear Science and Numerical Simulation*, Vol. 18, No. 10, 2013, pp. 2838-2851.
21. Öncü, S., J. Ploeg, N. Van de Wouw, and H. Nijmeijer. Cooperative Adaptive Cruise Control: Network-Aware Analysis of String Stability. *IEEE Transactions on Intelligent Transportation Systems*, Vol. 15, No. 4, 2014, pp. 1527-1537.
22. Zhao, S., and K. Zhang. A Distributionally Robust Stochastic Optimization-Based Model Predictive Control With Distributionally Robust Chance Constraints for Cooperative Adaptive Cruise Control Under Uncertain Traffic Conditions. *Transportation Research Part B: Methodological*, Vol. 138, 2020, pp. 144-178.
23. Flores, C., and V. Milanés. Fractional-Order-Based ACC/CACC Algorithm for Improving String Stability. *Transportation Research Part C: Emerging Technologies*, Vol. 95, 2018, pp. 381-393.
24. Li, F., and Y. Wang. Cooperative Adaptive Cruise Control for String Stable Mixed Traffic: Benchmark and Human-Centered Design. *IEEE Transactions on Intelligent Transportation Systems*, Vol. 18, No. 12, 2017, pp. 3473-3485.

25. Qin, Y., and S. Li. String Stability Analysis of Mixed CACC Vehicular Flow With Vehicle-to-Vehicle Communication. *IEEE Access*, Vol. 8, 2020, pp. 174132-174141.
26. Milanés, V., and S. E. Shladover. Modeling Cooperative and Autonomous Adaptive Cruise Control Dynamic Responses Using Experimental Data. *Transportation Research Part C: Emerging Technologies*, Vol. 48, 2014, pp. 285-300.
27. Hamdar, S. H., M. Treiber, H. S. Mahmassani, and A. Kesting. Modeling Driver Behavior as Sequential Risk-Taking Task. *Transportation Research Record: Journal of the Transportation Research Board*, 2008. 2088: 208-217.
28. Kahneman, D., and A. Tversky. Prospect Theory: An Analysis of Decision Under Risk. In *Handbook of the Fundamentals of Financial Decision Making: Part I* (MacLean, L. C., and W. T. Ziemba, eds.), World Scientific Publishing Co Pte Ltd, Singapore, 2013, pp. 99-127.
29. Hamdar, S. H. *Modeling Driver Behavior as a Stochastic Hazard-Based Risk-Taking Process*. PhD thesis. Northwestern University, Evanston, IL, 2009.
30. Treiber, M., A. Hennecke, and D. Helbing. Congested Traffic States in Empirical Observations and Microscopic Simulations. *Physical Review E*, Vol. 62, No. 2, 2000, p. 1805.
31. Kesting, A., M. Treiber, and D. Helbing. Enhanced Intelligent Driver Model to Access the Impact of Driving Strategies on Traffic Capacity. *Philosophical Transactions of the Royal Society A: Mathematical, Physical and Engineering Sciences*, Vol. 368, No. 1928, 2010, pp. 4585-4605.
32. Sharma, A., Z. Zheng, A. Bhaskar, and M. Haque. Modelling Car-Following Behaviour of Connected Vehicles With a Focus on Driver Compliance. *Transportation Research Part B: Methodological*, Vol. 126, 2019, pp. 256-279.
33. Li, Y., and H. Zhao. A Car-Following Model for Connected Vehicles Under the Bidirectional-Leader Following Topology. *Proc., 2017 IEEE 20th International Conference on Intelligent Transportation Systems (ITSC)*, Yokohama, Japan, IEEE, New York, October 16-19, 2017, pp. 1-5.
34. Liu, L., C. Li, Y. Li, S. Peeta, and L. Lin. Car-Following Behavior of Connected Vehicles in a Mixed Traffic Flow: Modeling and Stability Analysis. *Proc., 2018 IEEE 8th Annual International Conference on CYBER Technology in Automation, Control, and Intelligent Systems (CYBER)*, Tianjin, China, IEEE, New York, July 19-23, 2018, pp. 1085-1088.
35. Wang, S., B. Yu, and M. Wu. MVCM Car-Following Model for Connected Vehicles and Simulation-Based Traffic Analysis in Mixed Traffic Flow. *IEEE Transactions on Intelligent Transportation Systems*, 2021, pp. 1-8. https://doi.org/10.1109/TITS.2021.3052818.
36. Van Arem, B., C. J. Van Driel, and R. Visser. The Impact of Cooperative Adaptive Cruise Control on Traffic-Flow Characteristics. *IEEE Transactions on Intelligent Transportation Systems*, Vol. 7, No. 4, 2006, pp. 429-436.
37. Åström, K. J., and R. M. Murray. *Feedback Systems*. Princeton University Press, Princeton, NJ, 2010.
38. HCM. Highway Capacity Manual. Transport Research Board, Washington, D.C., 2000.
39. Treiber, M., and A. Kesting. *Traffic Flow Dynamics: Data, Models and Simulation*. Springer-Verlag, Berlin, Heidelberg, 2013.
40. Sharma, A., Z. Zheng, J. Kim, A. Bhaskar, and M. M. Haque. Assessing Traffic Disturbance, Efficiency, and Safety of the Mixed Traffic Flow of Connected Vehicles and Traditional Vehicles by Considering Human Factors. *Transportation Research Part C: Emerging Technologies*, Vol. 124, 2021, p. 102934.
41. Ali, Y., Z. Zheng, M. M. Haque, M. Yildirimoglu, and S. Washington. CLACD: A Complete LAne-Changing Decision Modeling Framework for the Connected and Traditional Environments. *Transportation Research Part C: Emerging Technologies*, Vol. 128, 2021, p. 103162.

The authors are solely responsible for the content of the paper.